Fuzzy Logic Controller-Based Power Control of DFIG Based on Wind Energy Systems

Leulmi Rayane[1] iD, Lekhchine Salima [2] iD, Medoued Ammar[1] iD

[1] Department of Electrical Engineering, LES Laboratory, University of 20 August 1955-Skikda,21000.

[2] Department of Electrical Engineering, LGMM Laboratory, University of 20 August 1955-Skikda,21000.

(rayane.leulmi@univ-skikda.dz, slekhchine@yahoo.fr, amedoued75@yahoo.fr)

Corresponding author : Leulmi Rayane, 21000, Tel: +213 675747840, rayane.leulmi@univ-skikda.dz

Abstract—Using renewable energy sources is the best alternative to fossil fuels for our energy needs because they are constantly renewed in nature, and we often call them green energy technologies because they produce little or no pollution. The most widely used renewable energy sources today are solar power, hydroelectricity, biomass, geothermal energy, and wind power. The widespread use of wind turbines has prompted electrical engineering researchers to improve this transition and the quality of the power supply, as this is the most promising energy source for our needs. To increase the efficiency of wind power systems, points need to be exploited more closely. Maximum power therefore requires the use of maximum power point trackers (MPPT), which, by optimizing power output, are crucial to wind power systems. Our work aims to apply fuzzy logic control to continuously and independently control the reactive and active power generated by the Doubly-fed induction generator (DFIG) of the flow-oriented wind power system.

Keywords— Wind power system; DFIG; MPPT; PI; FLC.

I.

1.   Introduction

The use of renewable energies is nothing new. They have been exploited by mankind since the dawn of time. In the past, water mills, windmills, firewood, animal traction, and sailing boats all contributed to the development of humankind. They were an economic activity in their own right, particularly in rural areas, where they were as important and diversified as food production [1]. Energy consumption worldwide and in our own country continues to rise. Fossil fuels (oil, natural gas, coal, etc.) account for the majority of energy used in the world. Because of their widespread use, these sources may eventually run out and pose a serious threat to the environment. This threat is manifested mainly through pollution and global warming due to the greenhouse effect [2]. Faced with these problems, researchers are turning their attention to new forms of many "renewable" energy sources, including wind energy [3]. Wind energy is the most promising source of renewable energy. In the 1980s, wind turbine systems (WTS) were first developed with a few tens of kilowatts of electricity; currently, most wind turbines

are installed and continue to grow in size [4]. The majority of wind turbines in use today include a power supply for doubly fed induction generators (DFIG). They can so function in a broad range of wind speeds and harvest the most power feasible at each

speed. Its rotor circuit is connected to the grid through a power converter, while its stator circuit is directly connected to it. Because there is less power transfer between the grid and the rotor, the cost of the converter is lower than for stator-fed variable-speed wind turbines [5]. This is the primary cause of the high-power output that we have observed in this generator. The ability to modify the generating voltage at the connection point is the second justification [6].

In this context, this study is devoted to the robust control of a wind energy conversion system based on (DFIG), to increase the efficiency of this system. According to the literature, conventional controllers' significant damping and sluggish response times are two major problems. Consequently, the demand for sophisticated control techniques is rising [7]. Prior research has mostly concentrated on enhancing the dynamics of conventional controllers, such as Fuzzy logic control (FLC) [9], backstepping control [8], and sliding mode control [8]..

This work presents the use of a modern (fuzzy) and classical (PI) control technique to a doubly-feed induction generator (DFIG) based variable-speed wind energy conversion system.
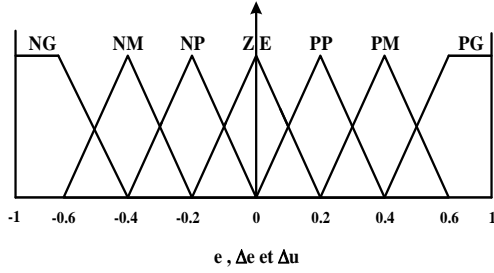
The comparison results of the simulation show how well the recommended control performed both dynamically and robustly when the FLC was used to track the reactive and active power of the reference stator.

This work is organized into four sections: The wind energy system employing the DFIG is described in Section 1; Section 2 models the system under study; Section 3 uses the PI and fuzzy logic controllers to control the turbine speed through Maximum Power Point Tracking (MPPT) technology, and section 4 controls the reactive and active power of the WECS.

2. Wind System Design Studied

There are several types of wind generators based on the asynchronous machine [10]. In our case, we give the structure of the wind generator based essentially on DFIG.

The wind energy system based on the DFIG is primarily composed of three components: the wind turbine, which is a mechanical component, DFIG, the electrical component, and two control components, Grid-Side control, and Rotor-Side control.

Fig.1. DFIG-based wind turbine design.

3. Modelling A Wind Power System

3.1. Wind Modeling

The following expression presents the wind profile:

$V(t) = 7 + 0.3 * \sin(0.1047 * t) + 0.3 * \sin(0.2665 * t) + 0.3 * \sin(1.293 * t) + 0.3 * \sin(3.6645 * t) + 0.3 * \sin(0.93275 * t) + 0.3 * \sin(4.3365 * t) + 0.3 * \sin(12.82575 * t) + 0.3 * \sin(3.264625 * t) + 0.3 * \sin(15.17775 * t)$ (1)

3.2. Turbine Modeling

Wind turbine power can be expressed as follows [11]:

$P_{\text{Wind tutbine}} = Cp. P_w = Cp(\lambda, \beta). \frac{\rho V^3 S}{2}$ (2)

With,
λ: Speed ratio
V: Wind speed.

R: Blade length.

S: Swept area of wind turbine.
β: Angle of blade orientation.
ρ: Air density.

The speed ratio is provided by [12]:

$$\lambda = \frac{\Omega_{turb}.R}{V_{vent}}$$ (3)

The power coefficient is provided by [12]:

$$C_p(\lambda, \beta) = C_1 - C_2(\beta - C_3).\sin(A) - C_4(\lambda - C_5)(\beta - C_3)$$ (4)

3.3. Modeling the DFIG

3.3.1. Electrical Equations [13]

$$\begin{bmatrix} V_{as} \\ V_{bs} \\ V_{cs} \end{bmatrix} = \begin{bmatrix} R_s & 0 & 0 \\ 0 & R_s & 0 \\ 0 & 0 & R_s \end{bmatrix} \begin{bmatrix} i_{as} \\ i_{bs} \\ i_{cs} \end{bmatrix} + \frac{d}{dt} \begin{bmatrix} \varphi_{as} \\ \varphi_{bs} \\ \varphi_{cs} \end{bmatrix}$$ (5)

$$\begin{bmatrix} V_{ar} \\ V_{br} \\ V_{cr} \end{bmatrix} = \begin{bmatrix} R_r & 0 & 0 \\ 0 & R_r & 0 \\ 0 & 0 & R_r \end{bmatrix} \begin{bmatrix} i_{ar} \\ i_{br} \\ i_{cr} \end{bmatrix} + \frac{d}{dt} \begin{bmatrix} \varphi_{ar} \\ \varphi_{br} \\ \varphi_{cr} \end{bmatrix}$$ (6)

With,
$[V_{as} V_{bs} V_{cs}]^T$, $[V_{ar} V_{br} V_{cr}]^T$: stator and rotor voltage vectors.
$[i_{ar} i_{br} i_{cr}]^T$, $[i_{as} i_{bs} i_{cs}]^T$: rotor and stator currents vectors.
$[\varphi_{ar} \varphi_{br} \varphi_{cr}]^T$, $[\varphi_{as} \varphi_{bs} \varphi_{cs}]^T$: rotor and stator voltage vectors.
R_s, R_r : stator and rotor resistance respectively.

3.3.2. Magnetic Equations [13]

$$\begin{bmatrix} \varphi_{as} \\ \varphi_{bs} \\ \varphi_{cs} \end{bmatrix} = \begin{bmatrix} L_s & M_s & M_s \\ M_s & L_s & M_s \\ M_s & M_s & L_s \end{bmatrix} \begin{bmatrix} i_{as} \\ i_{bs} \\ i_{cs} \end{bmatrix} + [M_{sr}] \begin{bmatrix} i_{ar} \\ i_{br} \\ i_{cr} \end{bmatrix}$$ (7)

$$\begin{bmatrix} \varphi_{ar} \\ \varphi_{br} \\ \varphi_{cr} \end{bmatrix} = \begin{bmatrix} L_r & M_r & M_r \\ M_r & L_r & M_r \\ M_r & M_r & L_r \end{bmatrix} \begin{bmatrix} i_{ar} \\ i_{br} \\ i_{cr} \end{bmatrix} + [M_{sr}] \begin{bmatrix} i_{as} \\ i_{bs} \\ i_{cs} \end{bmatrix}$$ (8)

With,
L_S: The inductance of the stator.
M_S: Mutual inductance in the phases of the stator.
L_r: The inductance of the rotor.
M_r: Interphase mutual inductance in a rotor.

3.3.3. Mechanical Equations [13]

$J\frac{d\Omega}{dt} = T_{em} - T_r - (f_r. \Omega)$ (9)
$\Omega = \frac{w}{p}$ (10)

Where :
Ω: The mechanical angular velocity.
T_{em}: Electromagnetic torque.
T_r: Resistive torque.
f_r: The coefficient of friction.
w :Electrical angular speed of rotor rotation.
J: The rotor's moment of inertia.
P: Number of pole pairs.

4. Control Strategy for A Variable-Speed Wind Turbine

In this work, we use MPPT control with mechanical speed feedback. The turbine speed must continuously adapt to the wind speed to optimize the amount of power generated by wind. For λ_{opt} and $\beta=2°$, the turbine's optimal mechanical speed is found. The generator speed serves as a reference for the PI controller. The latter adjusts the setpoint

The control is the electromagnetic torque T_{em}, it is used to turn the generator at its fastest possible pace. The torque that the controller computes produce the reference torque for the turbine model, as presented in Fig. 2.

Fig.2. Block schematic of power extraction maximization with speed control.

4.1. Speed control by Proportional-integral Controller (PI)

The electromagnetic torque is written as following [14]:

$$T_{em}^* = Reg(\Omega_{méc}^* - \Omega_{méc}) \tag{11}$$

$$\Omega_{méc}^* = G.\Omega_{turb}^* \tag{12}$$

Where,
Ω_{turb}^*:Reference turbine speed
Ω^*_{mec}: Reference mechanical speed
$\Omega_{méc}$: mechanical speed

$$\Omega_{turb}^* = \frac{\lambda_{opt}.V}{R} \tag{13}$$

Fig.3. Loop diagram for speed control using a PI controller.

The function for open-loop transfers is provided by [14]:

$$G_{BO} = \frac{\Omega}{\Omega^*} = \frac{k_{pw}.s+k_{iw}}{J.s^2+f.s} \tag{14}$$

We calculate a second-order transfer function in a closed loop. [15]:

$$G_{BF} = \frac{\Omega}{\Omega^*} = \frac{\frac{k_{pw}.s+k_{iw}}{J}}{s^2+\frac{k_{pw}+f}{J}.S+\frac{k_{iw}}{J}} \tag{15}$$

Whose canonical form is [14]:

$$G(s) = \frac{2.\xi.w_n.s+w_n^2}{s^2+2.\xi.w_n.s+w_n^2} \tag{16}$$

With, ξ represents the damping coefficient and w_n the natural pulsation.

The expressions for parameters k_{pw} and k_{iw} [14]:
$$\begin{cases} k_{pw} = 2.\xi.w_n.J - f \\ k_{iw} = J.w_n^2 \end{cases} \tag{17}$$

4.2. Basic Structure of a Fuzzy Controller

Linguistic variables play a very important role in fuzzy logic [9]. In our case, Wind is a linguistic variable if its values are: Strong, Medium, or Low.

Fig.4. linguistic variable with three linguistic terms.

Fig.5. Block diagram of a FLC.

➤ The knowledge base comprises a database that provides the information required for standardized functions, and a rule base that constitutes a set of linguistic expressions built around expert knowledge [9].
➤ Fuzzification is the process that makes it possible to go from numerical (physical quantities) to symbolic (fuzzy variables) [9].
➤ Inference rules: we used the two-dimensional matrix inference rule method with the Max-Min method

(Mamdani Implication) as shown in Fig.6.

Fig.6. Membership operations.

Table 1. Matrix of inference.

e \ Δe	NG	NM	NP	ZE	PP	PM	PG
NG	NG	NG	NG	NG	NM	NP	ZE
NM	NG	NG	NG	NM	NP	ZE	PP
NP	NG	NG	NM	NP	ZE	PP	PM
ZE	NG	NM	NP	ZE	PP	PM	PG
PP	NM	NP	ZE	PP	PM	PG	PG
PM	NP	ZE	PP	PM	PG	PG	PG
PG	ZE	PP	PM	PG	PG	PG	PG

➢ Defuzzification interface: It involves turning the hazy data produced by the inference mechanism into a physical quantity. Several methods have been developed to define the process control law [15]. In this work, we have used the center of gravity method. The center-of-gravity method Δ_{un} determined:

$$\Delta_{un} = \frac{\int x\mu(x)d_x}{\int \mu(x)d_x} \qquad (18)$$
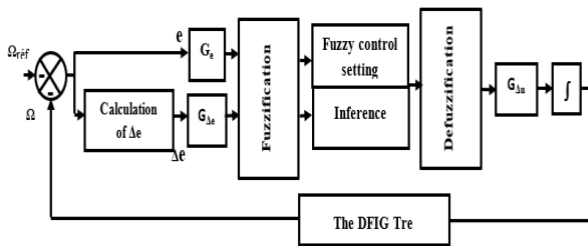
Fig.7. Block diagram of a FLC.

➢ The law of control:

The error and its variation determine the control law by following:

$$U_{k+1} = U_k + G\Delta_U.\Delta_{Uk+1} \qquad (20)$$

We normalize the error e and its variation, Δe, in the following ways:

$$\begin{cases} X_e = G_e.e \\ X_{\Delta e} = G_{\Delta e}.\Delta e \end{cases} \qquad (21)$$

5. Active And Reactive Power Control

Stator voltages along the (d-q) axis presented by [16]:

$$\begin{cases} i_{ds} = \frac{\varphi_s}{L_s} - \frac{M}{L_s}.i_{dr} \\ i_{qs} = -\frac{M}{L_s}.i_{qr} \end{cases} \qquad (22)$$

Active and reactive powers are presented by [16]:

$$\begin{cases} P_s = -V_s.\frac{M}{L_s}.i_{qr} \\ Q_s = V_s.\frac{\varphi_s}{L_s} - V_s.\frac{M}{L_s}.i_{dr} = \frac{V_s^2}{w_s.L_s} - V_s.\frac{M}{L_s}.i_{dr} \end{cases} \qquad (23)$$

The relationship between rotor voltages and rotor currents is shown in the following equation [17]:

$$\begin{cases} V_{dr} = R_r.I_{dr} - g.\omega_s.\left(L_r - \frac{M^2}{L_s}\right).I_{qr} \\ V_{qr} = R_r.I_{qr} + g.\omega_s.\left(L_r - \frac{M^2}{L_s}\right).I_{dr} + g.\omega_s.\frac{M^2.V_s}{w_s.L_s} \end{cases} \qquad (24)$$

5.1. Proportional-Integral (PI) Controller Synthesis
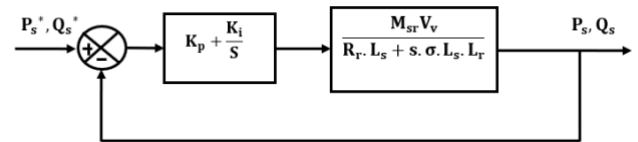
Fig.8. Block diagram of PI control structure.

The open-loop transfer function (OLTF) with controllers is written as follows:

$$G_{BF}(s) = \frac{P_s}{P_s^*} = \frac{\frac{(k_p.s+k_i).M.V_s}{\sigma.L_r.L_s}}{s^2 + s.\frac{R_r.L_s+k_p.M.V_s}{\sigma.L_r.L_s} + \frac{k_i.M.V_s}{\sigma.L_r.L_s}} \qquad (25)$$

5.2. Fuzzy logic control synthesis

To apply this control to our system, we used the structure of indirect vector control with a Mamdani-type fuzzy controller.
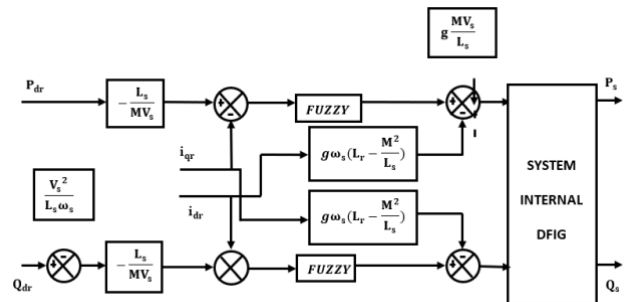
Fig.9. Block diagram of the FLC structure.

The rules of fuzzy logic control are presented in the following table.2:

Table 2. Fuzzy logic control rules.

e \ Δe	N	Z	P
N	GN	SN	SP
Z	GN	Z	GP
P	SN	SP	GP

6. Simulation Results

The results obtained by controlled simulation are presented and analyzed for blade orientation held constant at the minimum value (i.e. β = 2). In order to extract as much energy as possible, the speed ratio must be set at λopt= 9.41, which corresponds to the maximum value of the power coefficient Cpmax= 0.5268 whatever the wind speed.

We first used the MPPT structure with servo-control, mechanical speed by the following controllers: PI and fuzzy logic method. Figs 10 and 11 show the MPPT control with mechanical speed, such as: (Fig.10.a) mechanical speed and its reference, (Fig.10.b) error mechanical speed, (Fig.10.c) aerodynamic power, (Fig.10.d) relative speed and its reference. (Figure 11.a) mechanical speed and its reference, (Fig.11.b) error mechanical speed, (Fig.11.c) aerodynamic power, (Fig.11.d) relative speed and its reference.

Maximum power is achieved without overshoot; however, it should be noted that the instructions followed in transient and steady state are the same, albeit slightly modified.
On the other hand, the system response highlights both strategies, namely the fact that it follows the trajectory without any overshoot, including the best "Fuzzy logic" approach, according to the simulation results in Figures 10.b and 11.b.

We carried out simulations in MATLAB/Simulink to study the performance of a DFIG controlled by a FLC targeting power control.

Figure 12 Results of the FLC's power control simulation, including rotor current, stator current, torque, active power and its reference, and reactive power and its reference (Fig. 12.a,
12.b, and 12.c). We notice that the controlled quantities follow their reference trajectory, both the stator and rotor currents' waveforms are nearly sinusoidal, and the 3-Ø currents produced by the DFIG are proportionate to the active power supplied. The reactive and active powers precisely follow the references, are fully decoupled, and also have low static error.
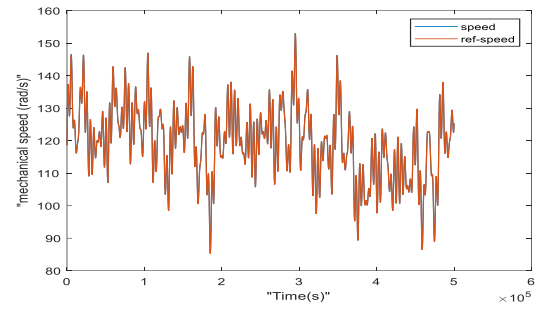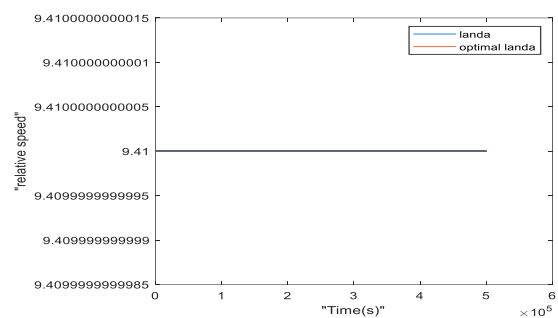

(a). Mechanical speed and its reference.
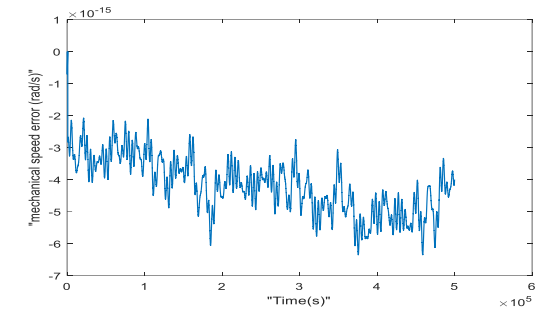
(b). Error mechanical.
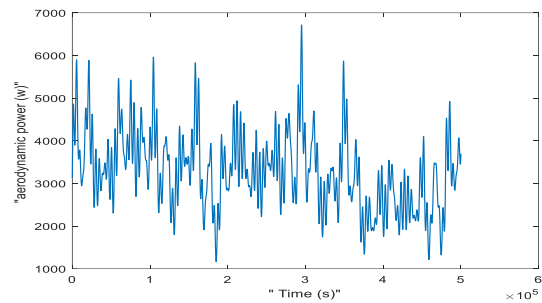
(C). Aerodynamic power.

(d). Relative speed and its reference.

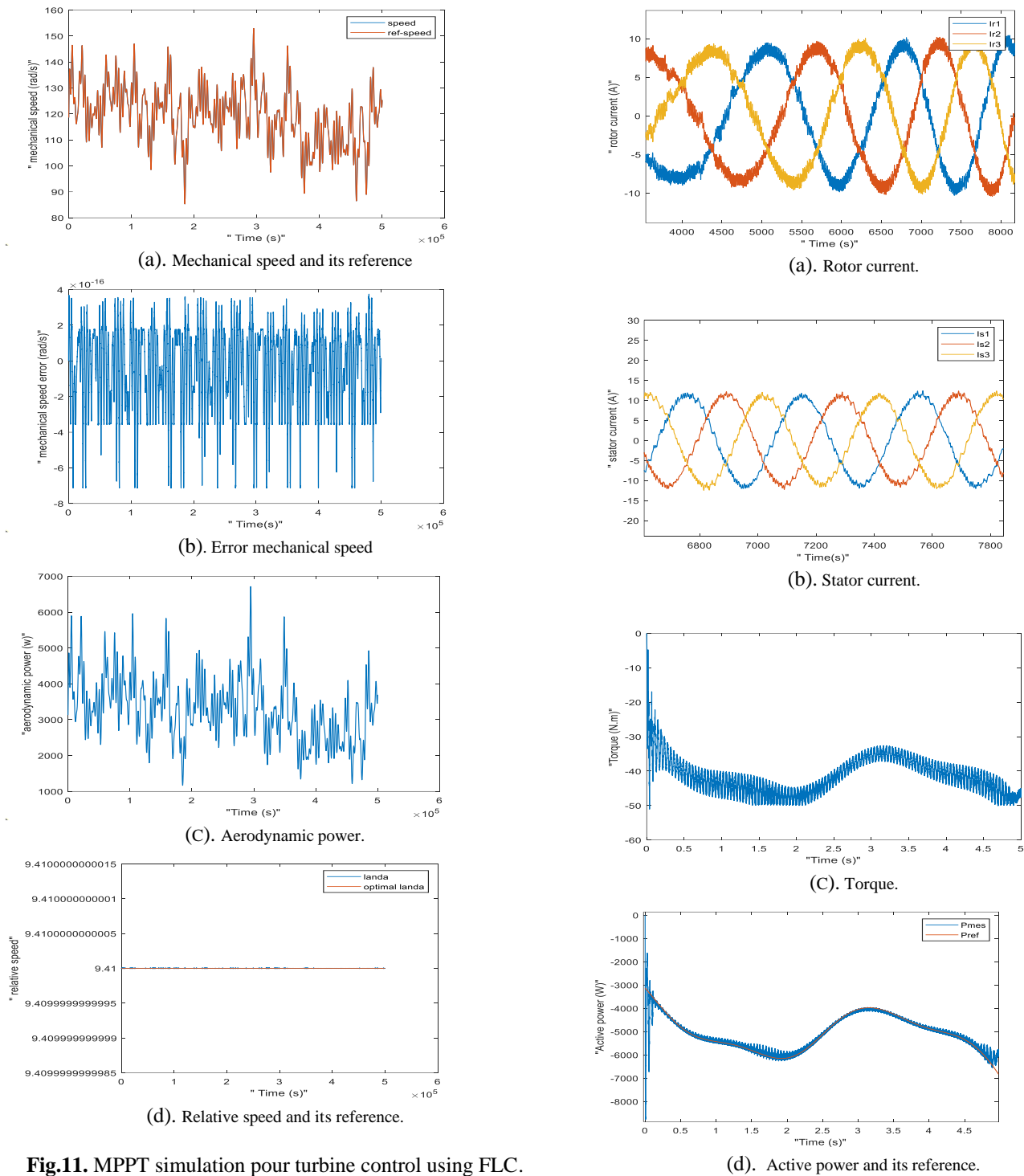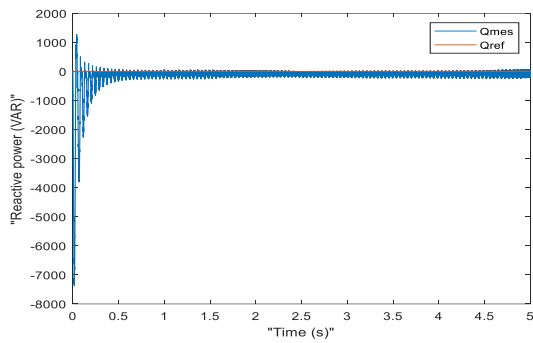**Fig.10.** MPPT simulation pour turbine control using PI.

(a). Mechanical speed and its reference

(b). Error mechanical speed

(C). Aerodynamic power.

(d). Relative speed and its reference.

Fig.11. MPPT simulation pour turbine control using FLC.

(a). Rotor current.

(b). Stator current.

(C). Torque.

(d). Active power and its reference.

(e). Reactive power and its reference.

Fig.12. Results of the FLC's power control simulation.

Conclusion

This article has demonstrated a DFIG-driven wind energy control system practicing PI and fuzzy logic. These two types of controllers are summarized and compared in the turbine part, about tracking, robustness, and reference. MATLAB/Simulink software has been utilized for analysis and validation of the results. The results of the simulation demonstrate the excellent dynamic performance and robustness of the suggested control when the FLC was utilized to monitor the reference stator's reactive and active power.

References

[1] J.M. Adànez, B.M. Al-Hadithi, A. Jiménez, "Wind turbine multivariable optimal control based on incremental state model,"Asian J control 20,1-13(2018).

[2] N.T. Anh Tuyet, S.Y. Chou, "Maintenance strategy selection for improving cost-effectiveness of offshore wind systems,"Energy Convers. Manag 157, 86-95 (2018).

[3] A. A. Chhipa, V. Kumar, S. Vyas, R. R. Joshi, " MPPT Optimisation Techniques and Power Electronics for Renewable Energy Systems", Wind and Solar Energy Systems. Int. J. Swarm Intell. 2021, 1, 1. [CrossRef]

[4] M. A. Akbari, J. Aghaei, and M. Barani, "Convex probabilistic allocation of wind generation in smart distribution networks," IET. Renew. Power. Gener, vol. 11(9), pp. 1211–8, 2017.

[5] N JargalsaikhanH Masrur A Iqbal S. Rangarajan S ByambaaT Senjyu, " A control algorithm to increase the efficient operation of wind energy conversion systems under extreme wind conditions " J. Int. Energy Reports. (8), 11429-11439 (2022).

[6] V. Kumar, A.S. Pandey, S.K. Sinha, "Grid integration and power quality issues of winnd and solar energy system," a review.In: International Confernece on Emerging Trends in Electrical, Electronics ans Sustainable Energy systems (ICETEESES-16), IEEE? 11-12 March 2016 (2016)

[7] M. Rajendran, L. A. Kumar, "Modeling and Simulation of a Dfig-Based Wind Energy System", In Lecture Notes in Electrical Engineering; Springer: Singapore, 2020; Volume 687, pp. 31–49.

[8] S. H. Lee, Y. J. Joo, J. Back, and J. H. Seo, "Sliding mode controller for torque and pitch control of wind power system based on PMSG," In: International Conference on Control, Automation and Systems, ICCAS, pp. 1079–1084, 2010.

[9] A. Z. Mohamed, M. N. Eskander, and F. A. Ghali, "Fuzzy logic control based maximum power tracking of a wind energy system," Renew. Energy, vol. 23, pp. 235–245, 2001.

[10] V. Sohoni, S. Gupta, & R. K. Nema, (2016), "A Critical Review on Wind Turbine Power Curve Modelling Techniques and Their Applications in Wind Based Energy Systems", Journal Of Energy, 2016, 1-18. https://doi.org/10.1155/2016/8519785

[11] A. M. Kassem, K. M. Hasaneen, & A. H. Yousef, (2013), "Dynamic modeling and robust power control of DFIG driven by wind turbine at infinite grid", International Journal Of Electrical Power & Energy Systems, 44(1), 375-382. https://doi.org/10.1016/j.ijepes.2011.06.038

[12] Y. Mousavi, G. Bevan, I. B. Kucukdemiral, & A. Fekih, (2022), "Sliding mode control of wind energy conversion systems : Trends and applications", Renewable & Sustainable Energy Reviews, 167, 112734. https://doi.org/10.1016/j.rser.2022.112734

[13] B. Yang, T. Yu, H. Shu, J. Dong, & L. Jiang, (2018), "Robust sliding-mode control of wind energy conversion systems for optimal power extraction via nonlinear perturbation observers", Applied Energy, 210, 711-723. https://doi.org/10.1016/j.apenergy.2017.08.027

[14] Y. Daili, J. P. Gaubert, L. Rahmani, A. Harrag, "Quantitativ feedback theory design of robust MPPT controller for small wind energy conversion systems: Design, analysis, and experimental study," Sustainable Energy Technologies and Assessments, vol. 35, pp 308-320, October 2019.

[15] H. Islam, S. Mekhilef, N. M. Shah, T. K. Soon, M. Seyedmahmousian, B., Horan, & A. Stojcevski, (2018), "Performance Evaluation of Maximum Power Point Tracking Approaches and Photovoltaic Systems", Energies, 11(2), 365. https://doi.org/10.3390/en11020365

[16] X. Pinghua, S. Dan, "Backstepping-based DPC strategy of a wind turbine-driven DFIG under normal and harmonic grid voltage," IEEE Trans. on P. Electron., 31(6), pp. 4216–25, 2016

[17] D. Houck, (2021), "Review of wake management techniques for wind turbines" Wind Energy, 25(2), 195-220. https://doi.org/10.1002/we.2668
.